Supporting Information

The Cooperation of Fe₃C Nanoparticles with Isolated Single Iron Atoms to Boost the Oxygen Reduction Reaction for Zn-Air Batteries

Fangling Zhou,[a,†] Peng Yu, [b,†] Fanfei Sun,[c] Guangying Zhang,[a] Xu Liu,[a] Lei Wang*[a]

[a] *Key Laboratory of Functional Inorganic Material Chemistry, Ministry of Education of the People's Republic of China, Heilongjiang University, Harbin, 150080, P. R. China*

[b] *Key Laboratory for Photonic and Electronic Bandgap Materials, Ministry of Education, School of Physics and Electronic Engineering, Harbin Normal University, Harbin, 150025, P. R. China*

[c] *Shanghai Synchrotron Radiation Facility, Shanghai Institute of Applied Physics, Chinese Academy of Sciences, Shanghai 201204, China.*

Corresponding authors. E-mail: wanglei0525@hlju.edu.cn
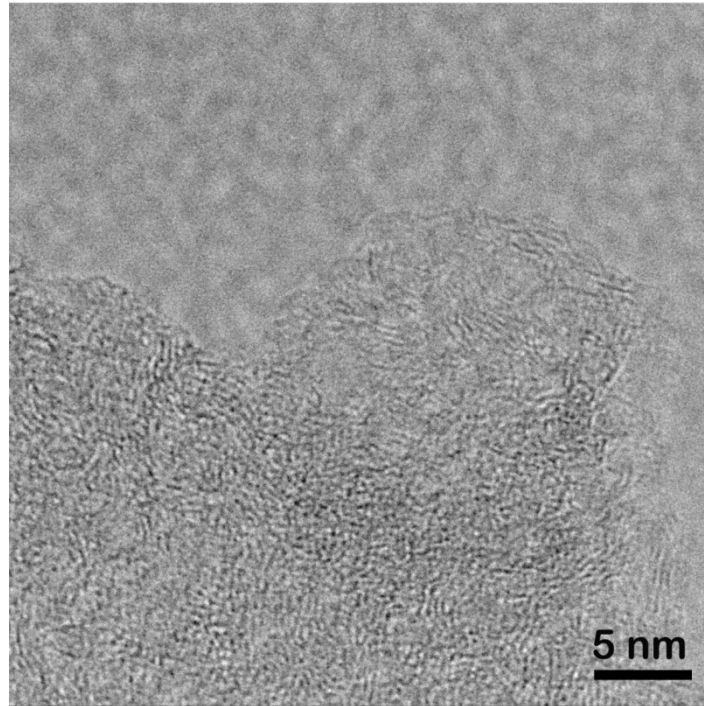
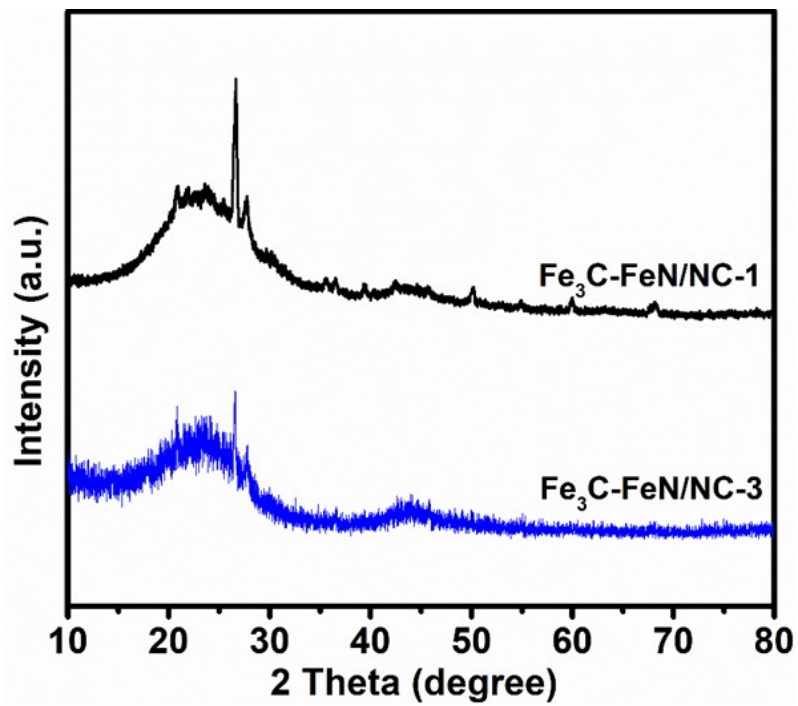[†]Equally contributed to this work.

Fig. S1. HRTEM image of Fe$_3$C-FeN/NC-2.

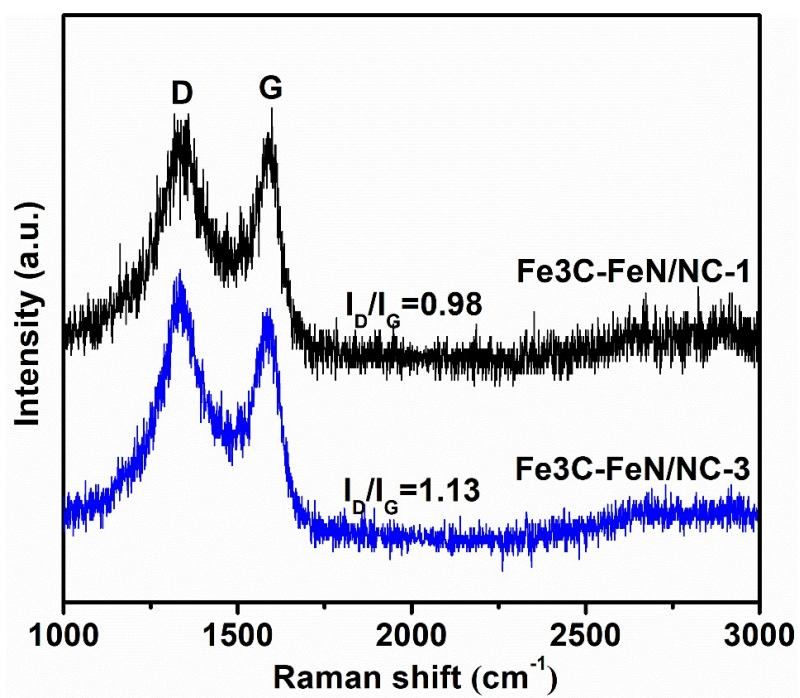**Fig. S2.** XRD patterns of Fe$_3$C-FeN/NC-1 and Fe$_3$C-FeN/NC-3.

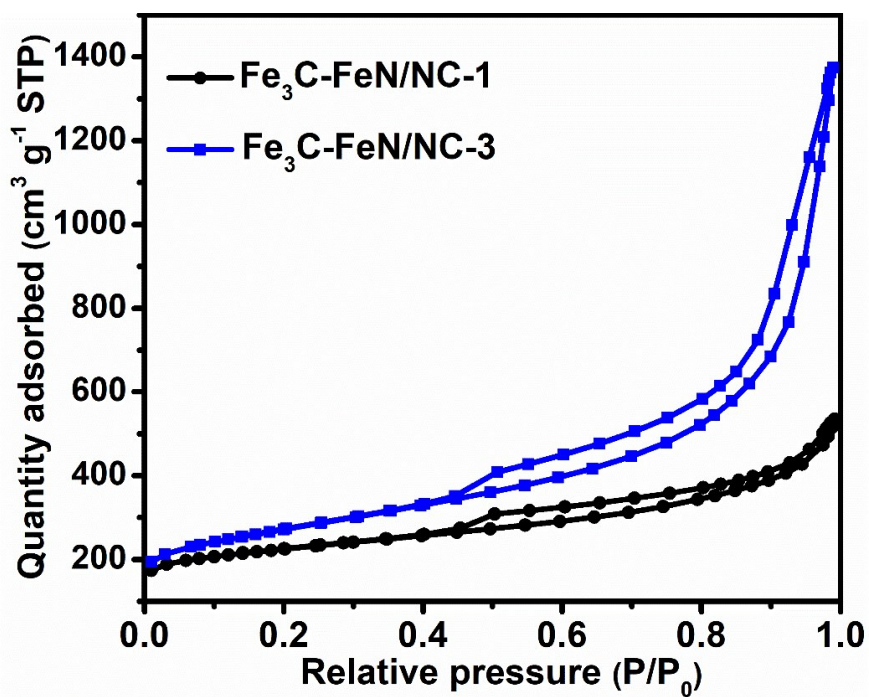**Fig. S3.** Raman spectra of Fe_3C-FeN/NC-1 and Fe_3C-FeN/NC-3.

Fig. S4. N_2 adsorption-desorption isotherms of Fe_3C-FeN/NC-1 and Fe_3C-FeN/NC-3.

Table S1. The comparison of BET specific surface area for all compared samples.

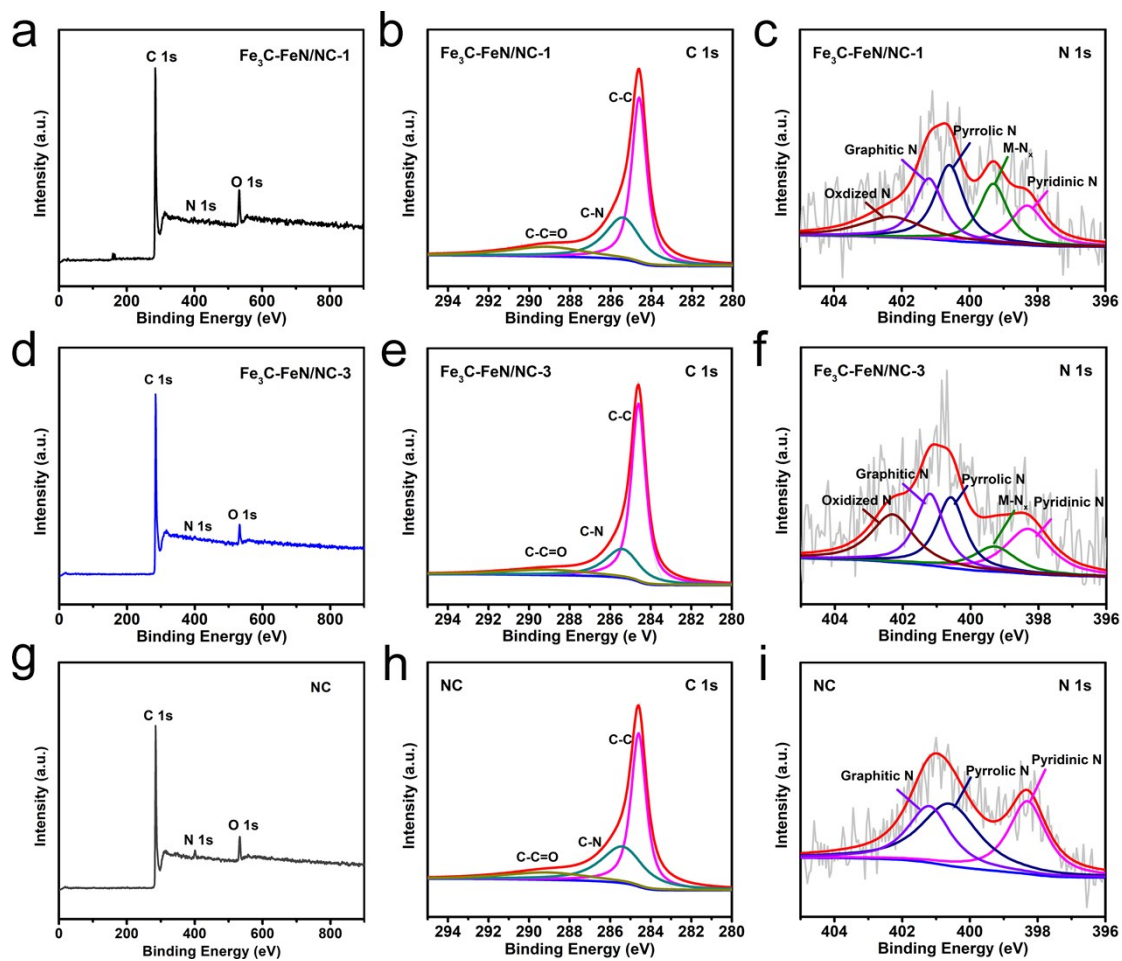| Samples	BET Surface Area ($m^2\,g^{-1}$)
Fe_3C-FeN/NC-1	781.8
Fe_3C-FeN/NC-2	853.1
Fe_3C-FeN/NC-3	954.3
Fe_3C/NC	344.4
NC	69.0

Fig. S5. a) Wide-scan, b) C 1s and c) N 1s XPS spectra of Fe₃C-FeN/NC-1. d) Wide-scan, e) C 1s and f) N 1s XPS spectra of Fe₃C-FeN/NC-3. g) Wide-scan, h) C 1s and i) N 1s XPS spectra of NC.
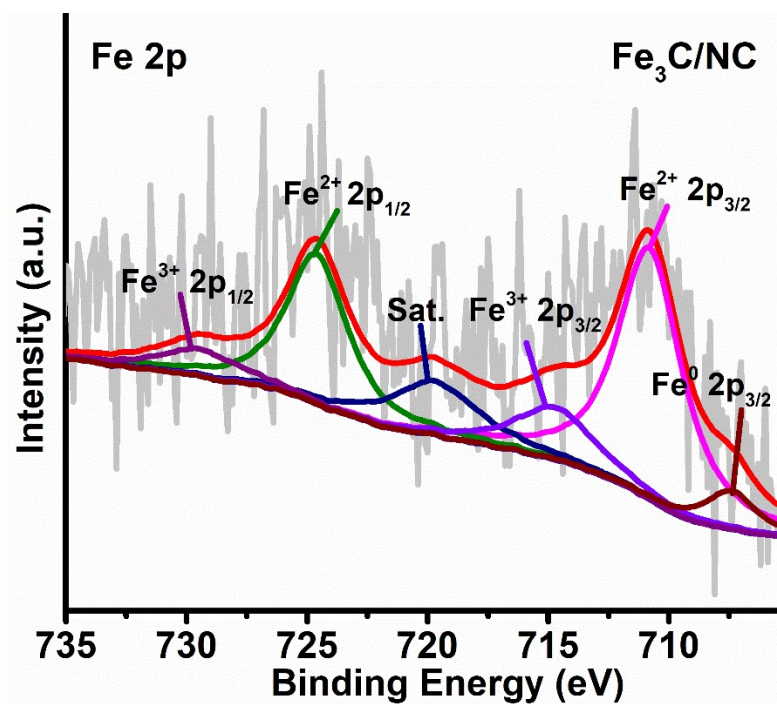
Fig. S6. Fe 2p XPS spectrum of Fe$_3$C/NC.
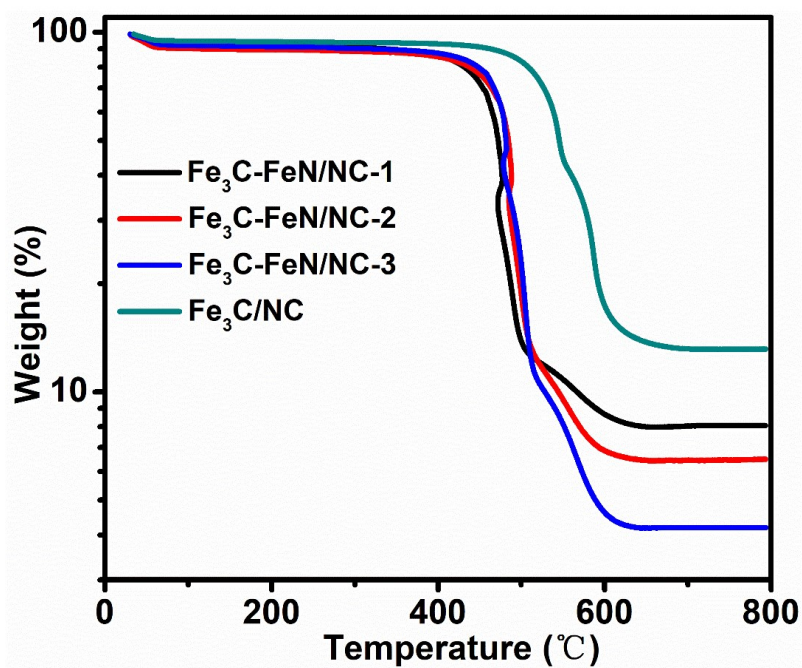
Fig. S7. Thermogravimetric curves of Fe$_3$C-FeN/NC-1, Fe$_3$C-FeN/NC-2, Fe$_3$C-FeN/NC-3 and Fe$_3$C/NC at air ambient.

Table S2. Fe contents for all compared samples calculated based on the TG analyses in Fig. S7.

sample	Final residual mass after TG tests Fe_2O_3 (wt. %)	Fe content calculated based on Fe_2O_3 (wt. %)
Fe$_3$C-FeN/NC-1	8.0	5.6
Fe$_3$C-FeN/NC-2	6.5	4.5
Fe$_3$C-FeN/NC-3	4.2	2.9
Fe$_3$C/NC	13.2	9.2

Table S3. EXAFS fitted results for Fe_3C-FeN/NC and Fe_3C/NC samples.

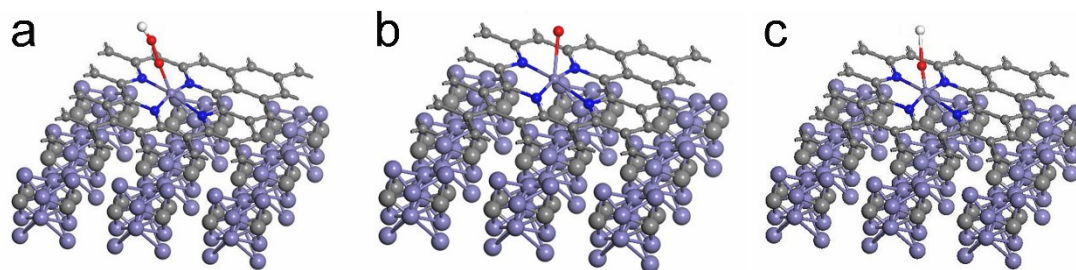| Sample	shell	N[a]	R (Å)[b]	σ^2 (10^{-3})[c]	E_0(eV)[d]	R factor
Fe$_3$C-FeN/NC-1	Fe-N	3.56 ± 0.2	1.97 ± 0.02	11.6	−6.9	0.002
	Fe-Fe	2.96 ± 0.3	2.54 ± 0.02	8.6	−5.4	
Fe$_3$C-FeN/NC-2	Fe-N	3.96 ± 0.2	1.94 ± 0.02	4.5	−4.5	0.003
	Fe-Fe	2.68 ± 0.2	2.53 ± 0.02	9.8	−5.7	
Fe$_3$C-FeN/NC-3	Fe-N	4.04 ± 0.2	1.99 ± 0.02	4.8	−5.7	0.002
	Fe-Fe	1.83 ± 0.2	2.52 ± 0.02	4.4	−3.8	
Fe$_3$C/NC	Fe-N	1.02 ± 0.2	1.91 ± 0.02	1.2	−4.6	0.002
	Fe-Fe	3.6 ± 0.2	2.44 ± 0.02	9.6	−9.4	

Fig. S8. The adsorption configurations for intermediates a) OOH*, b) O* and c) OH* on Fe_3C/Fe-N_4.
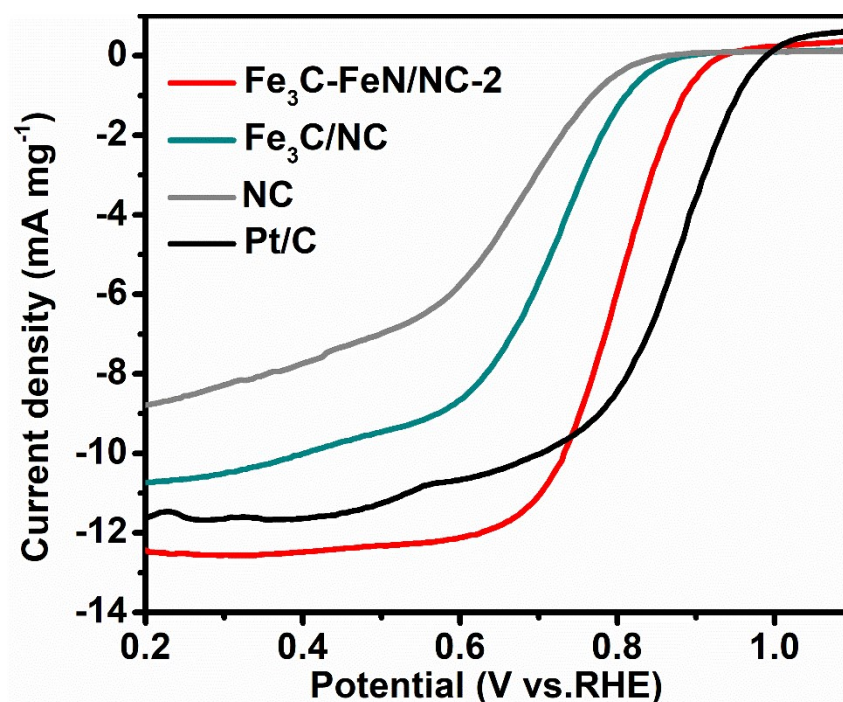
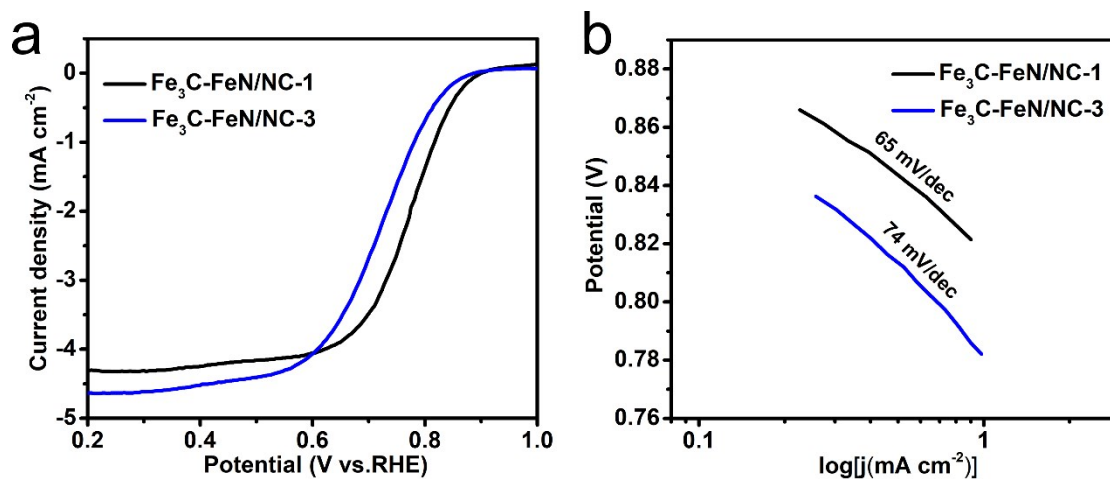**Fig. S9.** The mass activity for all the compared catalysts.

Fig. S10. a) ORR LSV curves and b) Tafel plots of Fe$_3$C-FeN/NC-1, Fe$_3$C-FeN/NC-3 tested in O$_2$-saturated 0.1 M KOH electrolyte.

Table S4. The comparison of ORR performance of Fe₃C-FeN/NC-2 with recently reported Pt-free catalysts tested in 0.1 M KOH electrolyte.

Catalyst	E_{onset} (V vs. RHE)	$E_{1/2}$ (V vs. RHE)	Tafel slope (mV dec^{-1})	Reference
P,S-Co$_x$O$_y$/Cu@CuS NW	0.89	0.67	80.8	S1
NiCo$_{2.148}$O$_4$ PNSs	0.85	0.65	-	S2
NiFe@N-CFs	0.94	0.82	58	S3
MnO/Co/PGC	0.95	0.78	69	S4
FeS/Fe$_3$C@NS-C-900	1.03	0.78	94	S5
Fe$_{0.5}$Ni$_{0.5}$@N-GR	0.94	0.83	-	S6
HNG-900	0.95	-	72	S7
Co$_2$P@CNF	0.915	0.803	77.1	S8
CoP@PNC-DoS	0.94	0.803	85.6	S9
Bi-CoP/NP-DG	0.93	0.81	-	S10
CoP-PBSCF	-	0.752	85.7	S11
NVG-30	0.91	0.80	51.1	S12
Fe$_3$C-FeN/NC-2	**0.95**	**0.80**	**55**	**This work**

References:

S1. T. L. L. Doan, D. T. Tran, D. C. Nguyen, D. H. Kim, N. H. Kim and J. H. Lee, *Adv. Funct. Mater.*, DOI:10.1002/admf.202007822.

S2. J. Yin, J. Jin, H. Liu, B. Huang, M. Lu, J. Li, H. Liu, H. Zhang, Y. Peng, P. Xi and C. H. Yan, *Adv. Mater.*, 2020, **32**, 2001651.

S3. Y. Niu, X. Teng, S. Gong and Z. Chen, *J. Mater. Chem. A*, 2020, **8**, 13725-13734.

S4. X. F. Lu, Y. Chen, S. Wang, S. Gao and X. W. D. Lou, *Adv. Mater.*, 2019, **31**, 1902339.

S5. Y. W. Li, W. J. Zhang, J. Li, H. Y. Ma, H. M. Du, D. C. Li, S. N. Wang, J. S. Zhao, J. M. Dou and L. Xu, *ACS Appl. Mater. Interfaces*, 2020, **12**, 44710-44719.

S6. P. Liu, D. Gao, W. Xiao, L. Ma, K. Sun, P. Xi, D. Xue and J. Wang, *Adv. Funct. Mater.*, 2018, **28,** 1706928.

S7. H. Cui, M. Jiao, Y.-N. Chen, Y. Guo, L. Yang, Z. Xie, Z. Zhou and S. Guo, *Small Methods*, 2018, **2,**1800144.

S8. J. Gao, J. Wang, L. Zhou, X. Cai, D. Zhan, M. Hou and L. Lai, *ACS Appl. Mater. Interfaces*, 2019, **11**, 10364-10372.

S9. Y. Li, Y. Liu, Q. Qian, G. Wang and G. Zhang, *Energy Stor. Mater.*, 2020, **28**, 27-36.

S10 J. Chen, B. Ni, J. Hu, Z. Wu and W. Jin, *J. Mater. Chem. A*, 2019, **7**, 22507-22513.

S11. Y.-Q. Zhang, H.-B. Tao, Z. Chen, M. Li, Y.-F. Sun, B. Hua and J.-L. Luo, *J. Mater. Chem. A*, 2019, **7**, 26607-26617.

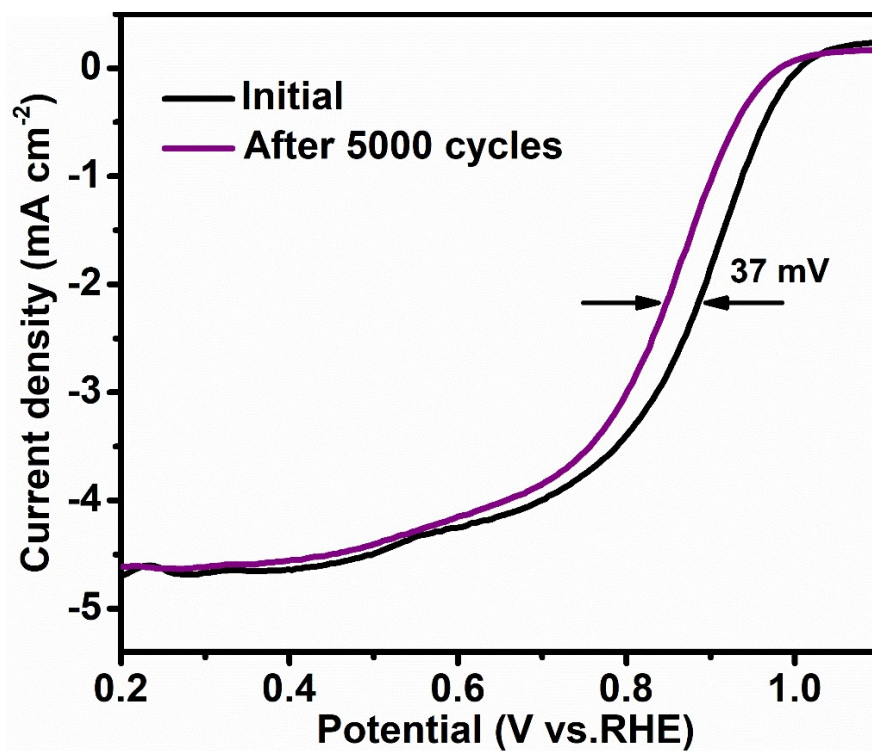S12. Z. Wu, Y. Zhang, L. Li, Y. Zhao, Y. Shen, S. Wang and G. Shao, *J. Mater. Chem. A*, 2020, **8**, 23248-23256.

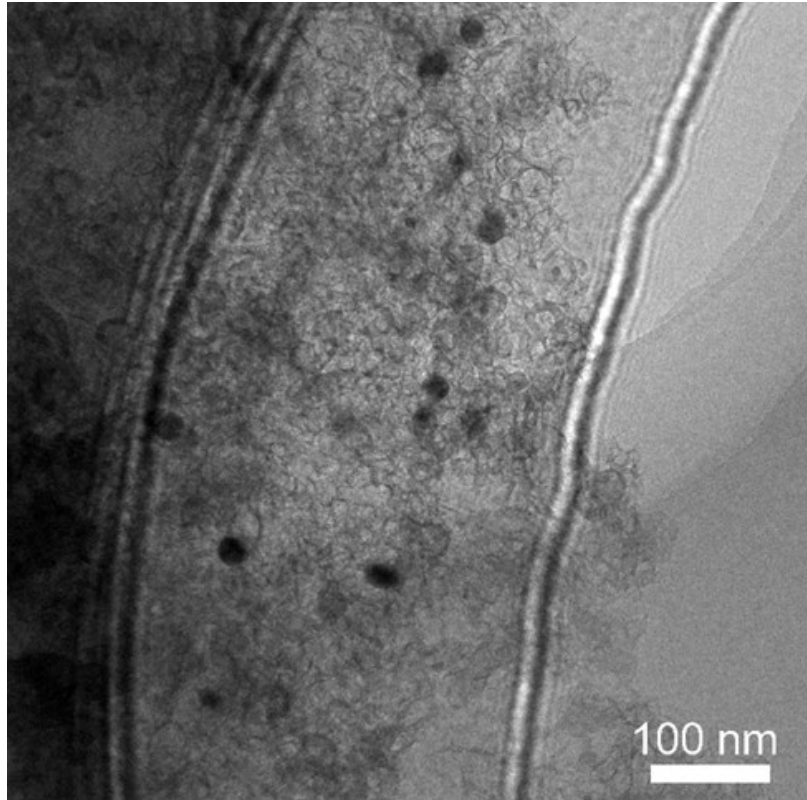**Fig. S11.** Stability test of the Pt/C catalyst after 5000 cycles.

Fig. S12. TEM image of Fe$_3$C-FeN/NC-2 after ORR test.

Density Functional Theory Calculations: All the theoretical computations were performed by CASTEP code (implemented in Material Studio). The generalized gradient approximation (GGA) with a Perdew–Burke–Ernzerhof (PBE) functional was used to describe the electronic exchange and correlation effects, and the plane-wave cutoff was tested and set to 340 eV. The selfconsistent field (SCF) tolerance was 1×10^{-5} eV. The Brillouin zone was sampled at a $(1 \times 1 \times 1)$ mesh. Fe_3C (211)and $Fe-N_4$-graphene (002) surface models were built based on the TEM and XRD results of the Fe_3C-FeN/NC catalysts.

The Gibbs free energy (G) was calculated as $G = E_{surf} + E_{ZPE} - T\Delta S$, where E_{surf} is the total energy calculated via DFT, and E_{ZPE} is the zero-point energy calculated using the vibrational frequencies of the adsorbates

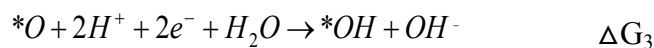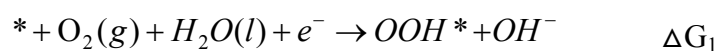The adsorption energy (E_{ads}) is defined as the following equation:

$$E_{ads} = E_{surf+O2} - E_{surf} - E_{O2}$$

Therein, $E_{surf+O2}$ is the total energy of the O_2/material system, E_{surf} is the material surface and E_{O2} is the free O_2 molecule.

Table S5. The calculated free energy of $Fe-N_4/Fe_3C$ with intermediates.

sample	Free energy (eV)
Clean surface	-42571.51
O*	-43004.97
OH*	-43023.09
OOH*	-43456.38

The ORR reaction for 4e⁻ pathway in alkaline media:

$$* + O_2(g) + H_2O(l) + e^- \rightarrow OOH* + OH^- \qquad \Delta G_1$$

$$OOH* + e^- \rightarrow O* + OH^- \qquad \Delta G_2$$

$$*O + 2H^+ + 2e^- + H_2O \rightarrow *OH + OH^- \qquad \Delta G_3$$

$$*OH + e^- \rightarrow * + OH^- \qquad \Delta G4$$

The Δ_{ZPE}, Δ_S and DFT-calculated free energy data are listed in **Table S5**. For each ORR reaction step, the Gibbs free energy of the formation can be calculated by ΔE is the reaction energy of a given reaction step and can be obtained from DFT calculations, ΔZPE and ΔS are the corrected zero point energy and entropy, respectively. U is the applied potential vs RHE and e is the charge transferred.

The Gibbs free energy of formation for each reaction step is calcutalted by the follows:

$$\Delta G = \Delta E_{DFT} + \Delta_{ZPE} - T\Delta S - e\,U + \Delta G_{pH}$$

Therein, the Zero point energies and entropic corrections ($\Delta_{ZPE} - T\Delta S$) are 0.30, 0.32 and 0.05 for OH*, OOH*, and O* species at 298 K, respectively. ΔG_{pH} is the correction of free energy of H^+, $\Delta G_{pH} = - k_b\,T\,\ln[H^+] = pH * k_b\,T\,\ln 10$.